Article

Allosteric Control of Photofoldamers for Selecting between Anion Regulation and Double-to-Single Helix Switching

Fred C Parks, Yun Liu, Sibali Debnath, Sydney R Stutsman, Krishnan Raghavachari, and Amar H Flood

J. Am. Chem. Soc., **Just Accepted Manuscript** • Publication Date (Web): 22 Nov 2018

J. Am. Chem. Soc.

Allosteric Control of Photofoldamers for Selecting between Anion Regulation and Double-to-Single Helix Switching

Fred C. Parks,[†] Yun Liu,[†,‡] Sibali Debnath,[†] Sydney R. Stutsman,[†] Krishnan Raghavachari,[†] and Amar H. Flood*[,†]

[†]*Department of Chemistry, Indiana University, 800 East Kirkwood Avenue, Bloomington, IN 47405, USA*

Abstract

Allosteric regulation of protein structure and function is a hallmark of biology. The structures of protein-like abiological foldamers have been subject to allosteric control, however, regulation of their function is rare. We report this behavior using a photoactive foldamer following the discovery that small and large anions select between single and double helical structures, respectively. Correspondingly, these anions activate different functions in the photofoldamer; small anions turn on photoregulation of anion concentrations while large anions turn on chiroptical switching of quaternary structure. For this demonstration, we used an aryl-triazole based photofoldamer in which the light-driven *trans-cis* isomerization of azobenzenes alters intrastrand π-π contacts while the triazoles define the allosteric anion-binding site. Binding to eleven anions of increasing size was quantified (Cl^-, Br^-, NO_2^-, I^-, NO_3^-, SCN^-, BF_4^-, ClO_4^-, ReO_4^-, PF_6^-, SbF_6^-). Contrary to expectations that single helices will expand to accommodate larger and larger guests, this behavior only occurs for smaller anions (Cl^- – NO_3^-; < 45 $Å^3$) beyond which the larger anions form double helices (SCN^- – SbF_6^-; > 45 $Å^3$). With small anions, the single helix regulates anion concentrations when the azobenzenes are photoswitched. The binding of large anions favors a chiral double helix and activates light-driven switching into racemic single helices thereby modulating the quaternary structure and chiroptical activity. This work shows how complex multifunctional outcomes emerge when allosteric changes in structure are expressed in intrinsically functional foldamers.

INTRODUCTION

Foldamers offer a powerful abiological platform for investigating the structures and functions common to biology.[1] Recent examples include structural emulation of DNA,[2] ribosomal synthesis,[3] and the hydrophobic collapse of proteins.[4] Allostery is a common biological character where the activity of an enzyme is altered by a change in its structure upon binding an allosteric effector.[5-8] Mimicry of this classic behavior has been expressed in supramolecular catalysis involving transition metals,[9-14] and has inspired modulations of molecular recognition where the binding of one guest (the effector) activates binding of a different guest.[15-21] With foldamers, allostery has inspired incorporation of other functions. In one case, the helix sense of transmembrane foldamers is photoswitched to alter enantiocatalysis.[22] In another, photoswitching of the foldamer between helix and random coil states produced an affinity swing to alter the solution concentration of chloride guests.[23] Nature also expresses other roles for which pyruvate kinase (PYK) is exemplary of a multifunctional protein.[24-25] It can exist in multiple quaternary forms (tetramers,[25-26] dimers,[27-28] and monomers[24, 29]) based on a variety of allosteric effectors[24-29] with each form having different functions. With fructose-1,6-bisphosphate[25, 29] bound, the tetramer is activated to catalyze formation of pyruvate. With triiodo-*L*-thyonine (T_3) binding as an effector, it drives formation of an active PYK monomer that homotropically regulates the concentration of T_3 in cells.[25-26, 29] The dimer is different again and phosphorylates proteins upon binding tyrosine phosphopeptide.[27-28] Different quaternary structures have different functions when activated by different allosteric effectors. We were surprised to find similar behavior emerge in a photofoldamer that derives multifunctional behavior from the allosteric binding of anions of different sizes (Figure 1).

This work was originally undertaken to investigate how the affinity swings of a photofoldamer are influenced by the size of the anionic guest. Based on prior anion-binding

foldamers,[30-31] we expected the helix to expand to accommodate larger guests to lower the affinity swing. Instead, and for the first time with aromatic foldamers, we found that guest size controls access to a single or double helix. We also found the different helices had different light-driven functions. Based on anion size, therefore, we activated either homotropic regulation of anion concentrations in solution, a behavior similar to PYK's T_3 regulation, or photoswitching between chiral double helices and racemic single helices. For this reason, we realized that these differences were similar to the complex multifunctional allostery displayed by PYK.

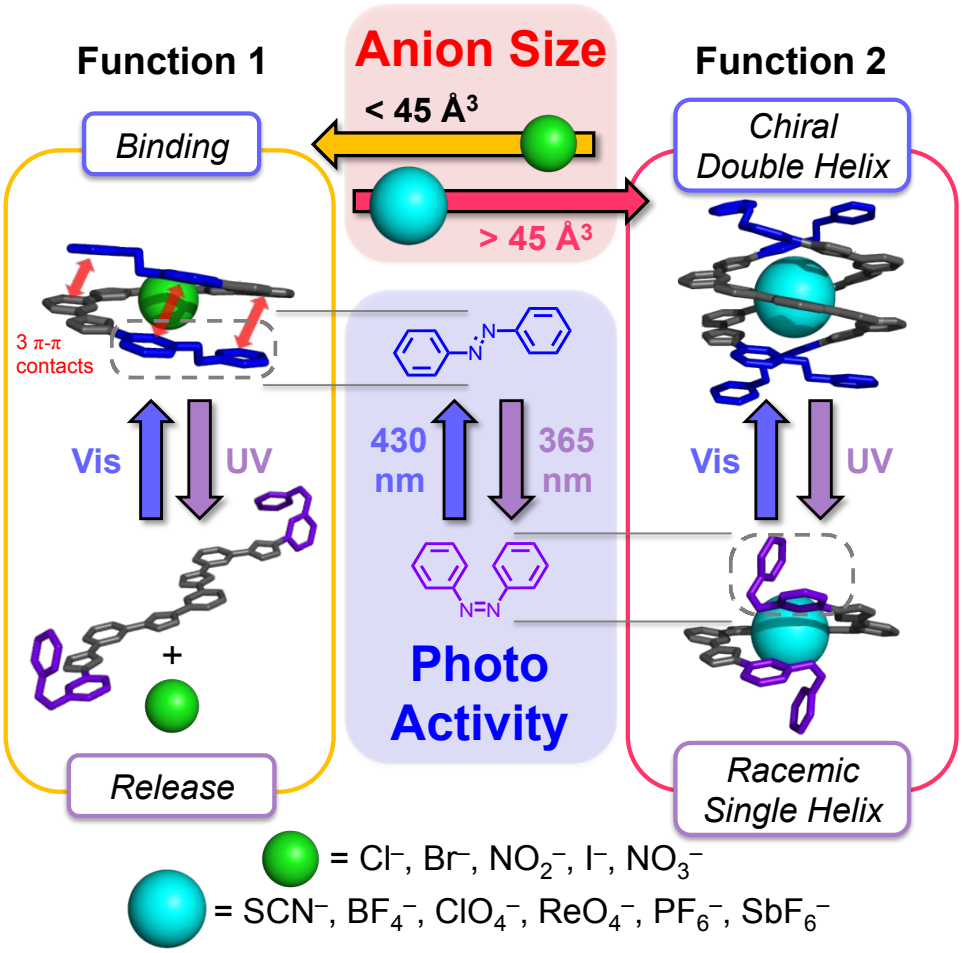

Figure 1. Guest size dictates selection of single or double helices and the function of the helices upon light switching of the azobenzene end groups. Under the working conditions, the single helix switches between *trans* ($\mathbf{F1}_{tt}$) and *cis* ($\mathbf{F1}_{cc}$) to drive cycles of anion binding and release whereas large anions allow switching between double and single helices.

We know that foldamers can respond to various stimuli to alter their structure. Folding into single helices can be driven using low temperature,[23, 32] poor solvents[4, 23, 32-36] and guest binding.[4, 32] Light-responsive photofoldamers[4, 23, 32-41] incorporate a covalently linked photoswitch,[42-47] like azobenzene.[33] Reversible activation of the photoswitch changes the conformational distribution of the foldamer to favor or disfavor the helix over the random coil. In prior work we coupled this helix-coil switching to the binding and release of anions,[23] an outcome gaining interest with photo-switchable receptors.[37, 48-57] Furthermore, even though we have observed a double helix with one photofoldamer,[4] the switching efficiency was poor.

Structural access to double helices instead of single helices requires additional considerations. Specific interactions between the intertwining strands can enhance double helix formation, such as with the coordination of transition metals.[58-60] External driving forces can be used, like solvophobic[61-62] and hydrophobic effects,[4, 63] in which double helices bury more of the total π surface than is possible in a single helix.[4] These solvent-driven effects benefit from structures with longer chains.[61] Torsion angles[64] can also be tuned to better accommodate the larger pitch present in the structures of double helices.[65] Finally, double helices can form around almost any guest (alkali[66-67] and transition-metal cations,[58, 60, 68] and anions[4, 69-71]). Returning to the role of guest size, anionic guests spanning a wide range of sizes (Cl^- to PF_6^- ranges 20 to 73 $Å^3$) have been studied with many foldamer classes, e.g., aryl-triazoles[4, 23, 30-32, 37, 72-76] indoles,[77-81] aliphatics,[82] and triazole-carboxamides.[83] However, the size of the bound guest has never been observed as a design feature for driving double helix formation despite studies directed at varying anion size.

Switchable foldamers that can interconvert reversibly between single and double helices have only been observed in three instances. Lehn used a Ag^+-templated double helix that formed

a single helix upon addition of cryptand, and was switched using acid/base addition to control Ag^+-cryptand binding.[84] Yashima used an activator-inhibitor[85] concept to unwind an oligoresorcinol double helix by addition of cyclodextrin and then re-wind upon addition of adamantane. Yamaguchi used thermally responsive oligomers to either denature[86] or form[87] double helices at elevated temperatures. Foldamers that switch reversibly between quaternary states using light as a non-destructive and non-invasive stimulus are not known.

Herein, we describe the unexpected selection of single and double helices from photofoldamers by using guest size, and the ability to use these guests as allosteric effectors to change the light-driven function of the photofoldamer (Figure 1). We demonstrate this finding with a flexible aryl-triazole foldamer **F1** (Scheme 1). Therein, the allosteric site is composed of triazole-based binding pocket and where the azobenzenes serve as functional sites. We selected 11 anions spanning volumes from 20 to 83 Å^3 and representing an array of geometries including spherical ($Cl^–$, $Br^–$, $I^–$) or pseudospherical ($BF_4^–$, $ClO_4^–$, $ReO_4^–$, $PF_6^–$, $SbF_6^–$), as well as linear ($SCN^–$), bent ($NO_2^–$), and trigonal planar ($NO_3^–$). In contrast to prior works by Jiang[31] and Craig[30] to bind foldamers with a wide range of anions, we first characterized the solvent-driven folding as a means to identify the best solvent for preparing a pre-folded initial state; acetonitrile in this case. Using a combination of NMR, circular dichroism (CD), and UV-Vis titrations, we characterize all binding constants for the helix and photoswitched random-coil states to identify how the function of the photofoldamer changes with anion size; we initially only expected to see changes in the affinity swing. Instead, these studies reveal that smaller anions (<45 Å^3, $Cl^–$ to $NO_3^–$) form single helices while larger anions (>45 Å^3, $SCN^–$ to $SbF_6^–$) form double helices with varying degrees of positive cooperativity[88] ($\alpha = 4\ K_{2:1} / K_{1:1} = 50 – 10{,}000$). Thus, we realized that small anions can activate the photofoldamer to change the free anion concentrations

(Function 1, Figure 1) as monitored using solution conductivity. This behavior was part of our original design.[48, 52-57, 89] With the larger anions, however, we activate a new chiroptical function in which the quaternary structure can be switched between chiral double helices and racemic single helices (Function 2, Figure 1) as seen by CD spectroscopy. This novel demonstration ultimately relies upon the use of an intrinsically functional photofoldamer in conjunction with the regulation of structure following the binding of allosteric effectors.

Scheme 1. Synthesis of foldamer **F1** via the arm-body approach.[a,b,c]

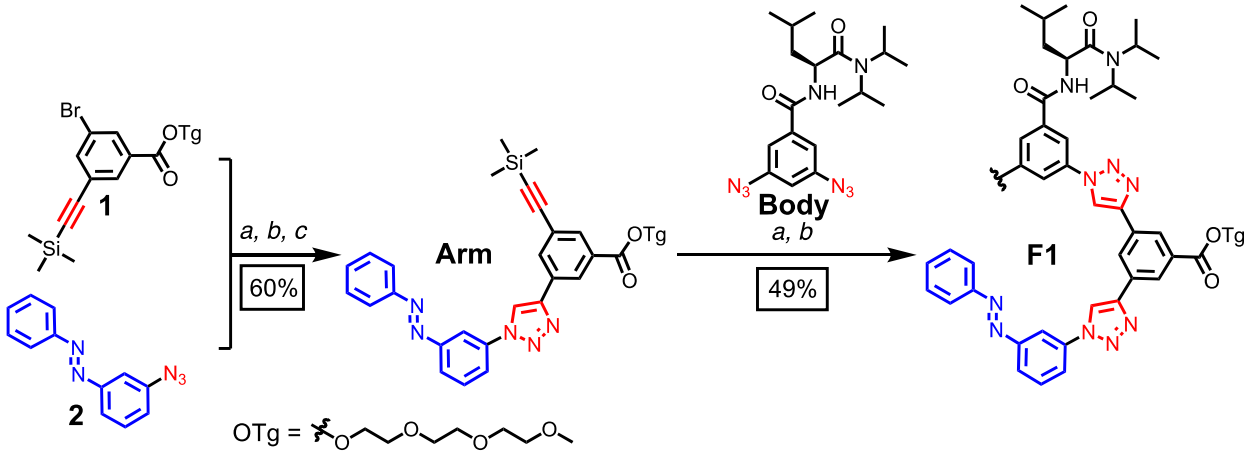

[a]Tetra-*n*-butylammonium fluoride, THF, acetic acid, 0 °C. [b]CuI, 1,8-diazabicyclo[5.4.0]undec-7-ene, toluene, 60 °C. [c]Trimethylsilylacetylene, CuI, $Pd(PPh_3)_2Cl_2$, triethylamine, THF, 60 °C.

RESULTS AND DISCUSSION

Molecular Design. The primary sequence of aryl and triazole residues in the C_2-symmetric photofoldamer **F1** (Scheme 1) is derived from prior designs.[23, 32] The current design is a configurational isomer in which the orientation of the triazoles is inverted. The east-west phenylenes are C-linked to the two neighboring triazoles rather than being N-linked, which enabled synthetic scalability. Azobenzene moieties provide an external means to control folding preferences using light.[23, 32] With both azobenzenes in their thermodynamically preferred *trans* (*t*) conformations in isomer $\mathbf{F1}_{tt}$, three π-π contacts (Figure 1) enhance the stability of the helical

conformation.[23] Once folded into a helix, the binding pocket is pre-organized for anion binding. Photoisomerization to the *cis* states lowers the π contact area to lower the helix-coil transition and thus reduce the foldamer's pre-organization and anion affinity. Finally, the chiral group on the central phenylene imparts handedness to the helix allowing CD spectroscopy to diagnose the extent of folding.

Foldamer Synthesis. Foldamer **F1** was synthesized in a straightforward manner using a body-arm approach (Scheme 1 and §S2). The **Body** was synthesized by installing the azide by the diazonium displacement of the amines on 3,5-diaminobenzoic acid with sodium azide,[90-91] followed by amide coupling with a chiral leucine derivative.[23] The **Arm** was synthesized by copper(I)-catalyzed azide-alkyne cycloaddition (CuAAC)[92-93] of 3-azidoazobenzene **2** with tri-substituted phenylene[94] **1** followed by thermal Sonogashira[95-96] reaction with trimethylsilylacetylene. Subsequent deprotection of the **Arm** and CuAAC with the **Body** in a 2:1 ratio afforded foldamer **F1** as a combination of isomers. Isolation of the *trans-trans* isomer (**F1**$_{tt}$) from *cis-trans* and *cis-cis* was accomplished by thermal isomerization of the azobenzenes in the dark. Compound identity was verified using 1D and 2D NMR spectroscopy (§S3), and high-resolution electrospray ionization mass spectrometry (HR-ESI-MS).

Photoisomerization of the azobenzenes from *trans* to *cis* using UV light (Figure 1) changes the folding propensity. The isomerization is not perfect with 20:80 ratios being typical.[97] Consequently, a total of three isomers are produced[23, 32] in the UV-based photostationary state (PSS) of the foldamer **F1**$_{\text{UV-PSS}}$: *trans-trans* (*tt*), *cis-trans* (*ct*), and *cis-cis* (*cc*). Each *cis* isomer results in removal of one of the three π-π contacts, shifting stability to the random coil[23] to lower the anion affinity of **F1**$_{\text{UV-PSS}}$.

Pre-organization of Foldamer F1. The helical folding of $\mathbf{F1}_{tt}$ was examined as a function of solvent quality[98] using CD spectroscopy (Figure 2a) to identify the ideal solvent to drive folding. The magnitude of the CD signal relates to both (Figure 2b) folding of the random coil into a helix and the preference of one twist sense over the other. Solvent quality was varied from least to most polar as constrained by compound solubility. The $E_T(30)$ scale[99] of polarity is generally applicable to solvophobic processes involving π systems.[100] We see (Figure 2a) that in solvents of modest polarity, such as THF, $CHCl_3$, and CH_2Cl_2 ($E_T(30) = 37 – 45$), there was no CD response. Starting from CH_2Cl_2, increases in the amount of MeCN from 20% to 100% ($E_T(30) = 42 – 46$) generated a continual increase in the CD signal (Figure 2a). This trend is consistent with solvophobic driving forces stabilizing the helix.[61, 101-102] Use of protic solvent mixtures by introduction of water, however, led to a decrease in the CD response likely arising from equalization between *P* and *M* helical preferences rather than from unfolding. To distinguish between these two options we measured the melting temperature and found an increase from $T_m = 32 \pm 2°C$ (Fig. S10) in pure MeCN to $T_m = 40 \pm 2°C$ (Fig. S11) upon the introduction of 10% H_2O. The higher melting temperature is consistent with water producing greater *P*-*M* equalization. Pure acetonitrile was chosen for subsequent studies to avoid the ambiguities of mixed solvents while maximizing the helical excess of the foldamer.

We also verified that the photoisomerized form of the foldamer, $\mathbf{F1}_{UV\text{-}PSS}$, is less able to support a helix than $\mathbf{F1}_{tt}$. The CD response of $\mathbf{F1}_{UV\text{-}PSS}$ (Fig. S83) was reduced even in pure acetonitrile. The residual peak at 270 nm of modest intensity was attributed to residual *trans*-*trans* form ($\mathbf{F1}_{tt}$, 16%) in the photostationary state. This CD response is consistent with a loss in the stability of the helix for the *cis*-*cis* and *cis*-*trans* isomers.

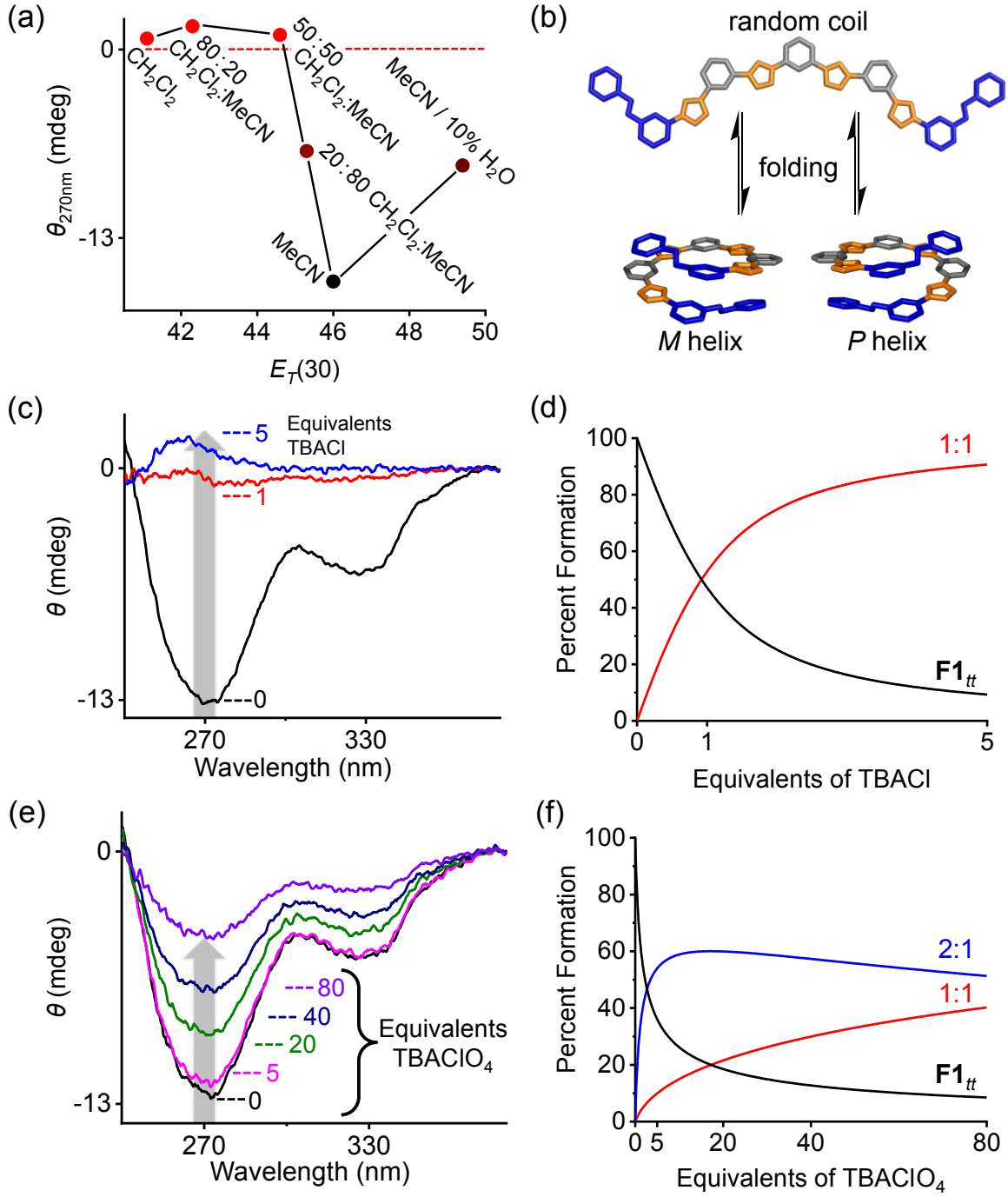

Figure 2. (a) Molar ellipticity (θ, mdeg) values at 270 nm of foldamer $\mathbf{F1}_{tt}$ (189 μM) in various solvent mixtures versus solvent polarity (E_T(30), kcal / mol). E_T(30) values of mixed solvents were determined with mole fractions. (b) Equilibrium between unfolded coil conformation and the chiral folded helices of $\mathbf{F1}_{tt}$. (c) CD titration of the $\mathbf{F1}_{tt}$ with TBACl ($\mathbf{F1}_{tt}$, 150 μM, CH_3CN, 0.05 cm, 298 K) and (d) the corresponding speciation curve (log $K_{1:1}$ = 4.1). Analogous (e) CD titration and (f) speciation model with $TBAClO_4$ (log $K_{1:1}$ = 2.6, log β_2 = 7.3).

Structural Allostery: Selection of Single and Double Helices. The selection of single or double helices using anionic guests of different sizes was identified from ^{1}H NMR (§S6) and CD (§S5) titrations. Smaller anions (<45 Å^3) favor single helices where binding of chloride is exemplary. ^{1}H NMR studies were conducted in dichloromethane (CD_2Cl_2) to resolve peaks and replicated in 20% acetonitrile in dichloromethane to enhance π stacking. All the titrations that were conducted in either dichloromethane or with 20% acetonitrile were used for structural and speciation determinations only. The foldamer shows continual peak shifts (Figure 4b) upon addition of chloride as the tetrabutylammonium (TBA^+) salt (Fig. S24), which is consistent with a 1:1 stoichiometry (Figure 3, yellow box). The internal protons (H^A, H^B, H^C, H^D) showed only downfield movements consistent with anion binding.[103-105] Protons on the azobenzenes showed upfield movements consistent with π stacking[106] arising from anion-induced folding into a helix.[107]

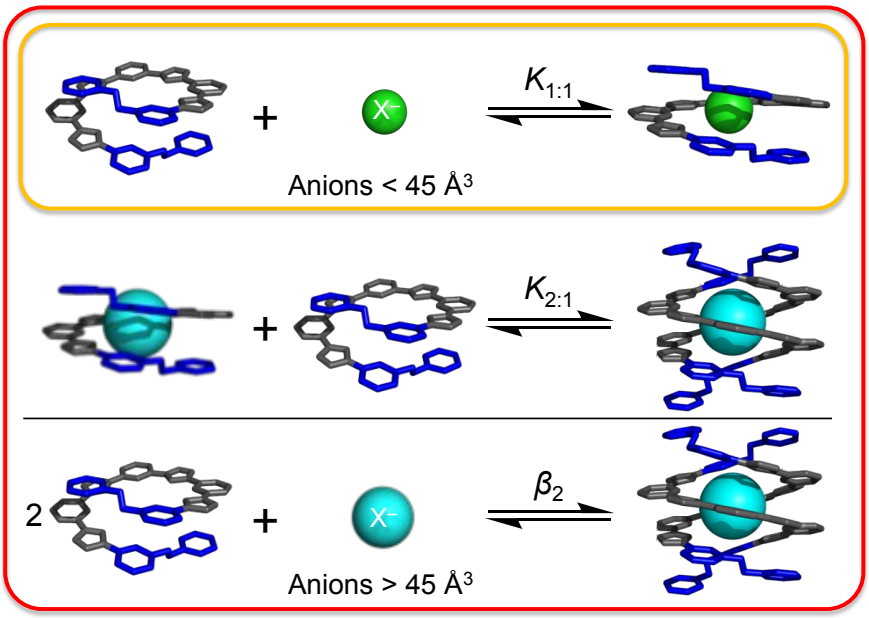

Figure 3. Binding equilibria involving small anions (yellow box) and large anions (red box).

Larger anions were discovered to produce double helices (Figure 3, red box). Perchlorate is exemplary. Even though π-stacking is less favored in dichloromethane, ^{1}H NMR signals for the double helices can still be seen (Fig. S42). Specifically, we see inflection points characteristic of 2:1 stoichiometries in protons H^C, H^D, and H^F, at 1, 3, and 1.5 equivalents (Fig. S43). Consistently, the double helix is dominant in the ESI-MS (Figure 4g, CH_2Cl_2, 0.1 mM) with 0.5 equivalents of $TBAClO_4$. This finding contrasts with Cl^- (Fig. S53a) where the 1:1 dominates. In this case, and based on our prior experience,[108-109] the ESI-MS only provides a qualitative assessment of the speciation preferences present in solution.

While large anions were studied previously with aryl-triazole foldamers,[30-31] it seems that the solvents used inhibited formation of double helices. Jiang[31] used a 10- and 20-residue foldamer with bisulfate (HSO_4^-) and phosphate ($H_2PO_4^-$), which should be large enough to generate a double helix. However, only a single helix was observed. Their studies were conducted in a 10:90 DMSO:THF mixture ($E_T(30) \sim 38$). The solution polarity falls into the regime (Figure 2a) where folding is disfavored. Craig[30] used an aryl-triazole 9-mer with a range of anions, including the large PF_6^- anion. In acetone ($E_T(30) = 42$), they only observed a single helix. Based on our observations here and the literature precedent,[30-31] anion size appears to cooperate with the solvophobic burial of π surfaces to drive double helix formation.

To approach conditions that favor folding (pure acetonitrile), but still retain sharp ^{1}H NMR peaks, a mixture of 20% acetonitrile in dichloromethane ($E_T(30) \sim 42$) was used. Double helix formation was enhanced (Figure 4e) over pure CD_2Cl_2. We expect and see that protons H^A, H^E and H^F are shifted upfield (Figure 4d) on account of being placed into a π-stacked environment (Figure 4e). By contrast, these same protons are not involved in π stacking in the single helix (Figure 4f) and do not show inflection points with chloride (Fig. S27). With

perchlorate, these protons show inflection points at 1.5, 1.75, and 6 equivalents (Figure 4c), respectively. After this point they shift downfield indicative of less π stacking in the single helix and eventual formation of the 1:1 species with excess anion. Of these, protons H^A, H^B, and H^E had not originally shown inflection points in the titration conducted in the less polar CD_2Cl_2. From the number of peaks in the ^1H NMR spectra (Figure 4c) and symmetry considerations, the 2:1 species is an intertwined double helix (Figure 4e) rather than a stacked pair of helices.

Anions that favor single helices can be identified from CD spectroscopy. Addition of one equivalent of chloride led to the loss in the CD response of $\mathbf{F1}_{tt}$ (150 μM, CH_3CN, Figure 2c), as observed[32] with related aryl-triazole foldamers. Presumably, stronger CH hydrogen bonding to the chloride ion disrupts the weak interactions that direct the chiral preferences of the uncomplexed helix. This outcome contrasts with helicity inversions seen by Jeong when binding anions to the single helix form of an indolocarbazole foldamer.[80, 110] Overall, single-helix 1:1 complexes lose their CD response upon addition of 1 equivalent of anion.[111]

In contrast to chloride, perchlorate shows almost no loss in CD signal intensity up to 5 equivalents (150 μM, CH_3CN, Figure 2e). This observation is consistent with the production of double helix (~60%) seen from the calculated speciation profile (Figure 2f). Presumably, chiral preferences are retained in the double helix as a result of intertwining.

CD titrations (§S5) were undertaken to differentiate between anions that promote single and double helices. The halides (Cl^-, Br^-, I^-), nitrite (NO_2^-) and nitrate (NO_3^-) all showed a drastic loss in the CD signal indicative of 1:1 single helices. Thiocyanate (SCN^-) showed a decrease in intensity (Fig. S18) but not to the extent of the halides, which is consistent with intermediate behavior. The larger anions (BF_4^-, ClO_4^-, ReO_4^-, PF_6^-, SbF_6^-) retained the CD

signal indicative of double helix formation. These results reveal size dependent outcomes with anions having a volume of 45 Å^3 or larger forming double helices.

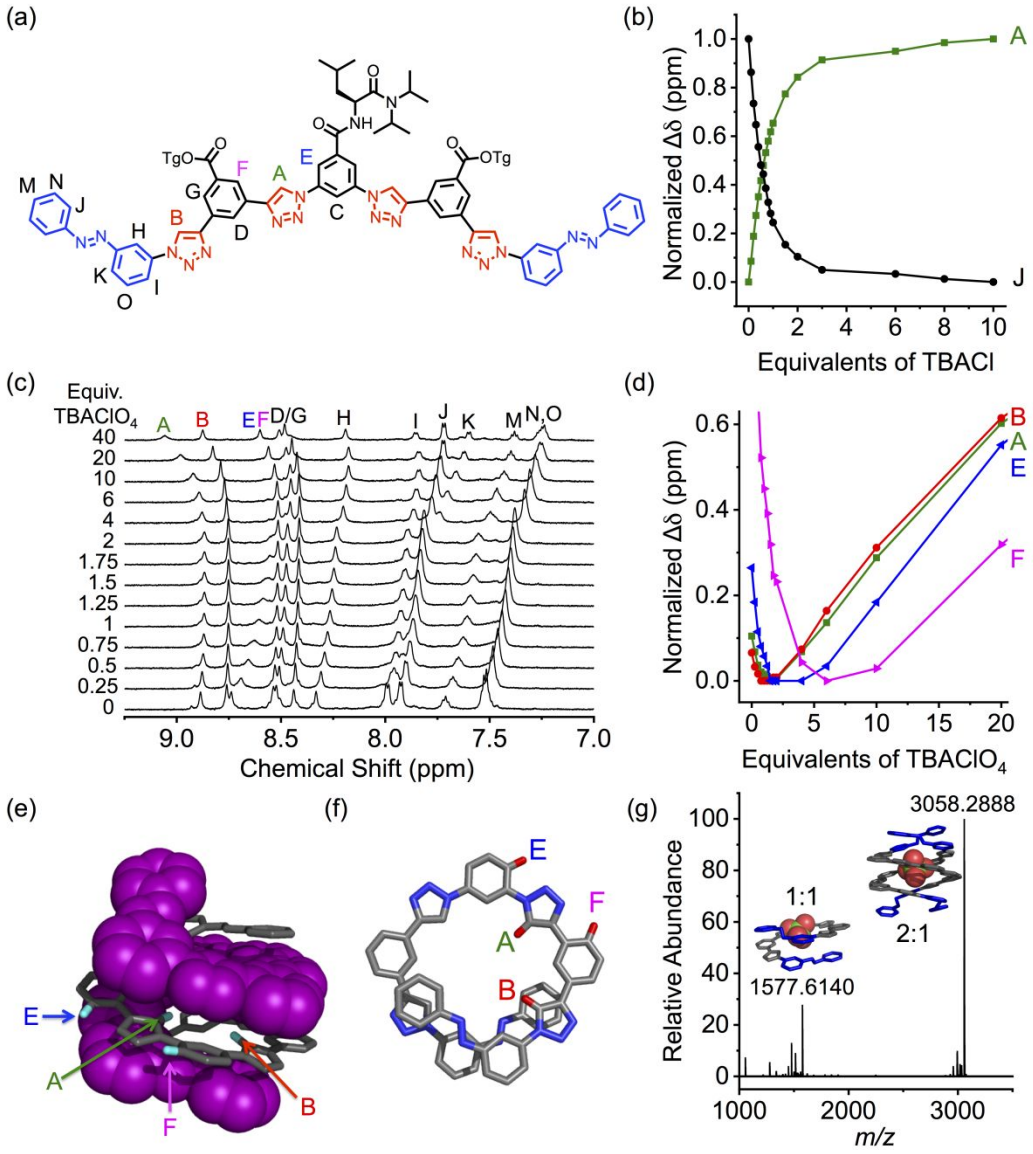

Figure 4. (a) Structure of foldamer **F1**$_{tt}$. (b) Normalized chemical shifts of H^A and H^J with TBACl additions (**F1**$_{tt}$, 1 mM, CD_2Cl_2, 298 K, 600 MHz). (c) ^{1}H NMR titration of $TBAClO_4$ with **F1**$_{tt}$ (1 mM) and the (d) normalized change in chemical shifts (H^A, H^B, H^E, H^F) with $TBAClO_4$ (20:80 CD_3CN:CD_2Cl_2, 298 K, 600 MHz). (e) DFT-optimized geometry of 2:1 double helix around ClO_4^- with H^A, H^B, H^E, and H^F labeled (ClO_4^- omitted for clarity) and (f) DFT-optimized geometry of the single helix around ClO_4^-;location of protons H^A, H^B, H^E, and H^F labeled (ClO_4^- omitted; ONIOM (B97D3/6-311+G(d):B97D3/6-31G(d)). (g) HR-ESI-MS of **F1**$_{tt}$ (0.1 mM) with 0.5 equivalents of $TBAClO_4$ (CH_2Cl_2).

Quantification of Anion Binding Affinities and Helix Stabilities. The anion affinities (Table 1) were measured in acetonitrile as a means to understand the recognition properties of the foldamer in its most pre-organized starting state. On account of broad NMR peaks in the titrations with acetonitrile (Figs. S28, S46), titrations were followed by UV-Vis spectroscopy (§S8). The stability constants were quantified using an equilibrium-restricted factor analysis as implemented in Sivvu.[112] Ion pairing was ignored on account of being negligible under the conditions examined (polar solvent and low concentration; see §S15). Binding equilibria involved formation of either single ($K_{1:1}$) or double helices ($K_{1:1}$, $K_{2:1}$, β_2) as indicated by the anion-induced CD responses and titrations. Consistently, inflection points in the UV-Vis titrations emerged (Fig. S76) for the anions predicted to form double helices. With SbF_6^-, an inflection point was seen at 0.5 equivalents while BF_4^-, ClO_4^-, and PF_6^- all had inflection points at 1.0 equivalents suggesting different levels of cooperativity. While UV absorbances of SCN^- and ReO_4^- anions precluded observation of inflections, they were seen in ^{1}H NMR titrations recorded in CD_2Cl_2. Therefore, SCN^-, BF_4^-, ClO_4^-, ReO_4^-, PF_6^- and SbF_6^- were fit to double helix binding models (Figure 3) while Cl^-, Br^-, I^-, NO_2^- and NO_3^- were restricted to 1:1 binding as a single helix.

Selectivity and Anion Affinity of F1$_{tt}$. We observed trends in the equilibrium constants associated with formation of single and double helices (Figure 5). Across the series of small anions that form single helices, there is poor anion binding selectivity. While there is no size selectivity across the halides, they are the preferred anions over the nitrogen oxides (NO_2^-, NO_3^-), suggesting a modest shape-based selectivity.

Across the larger anions that form double helices, we see a number of trends. The stabilities of the 1:1 single helices (Table 1, Figure 5) are seen to drop with increasing size of the

anions. This is true across the tetrahedral ions BF_4^-, ClO_4^-, and ReO_4^- (53 – 60 Å^3) and for the two octahedral anions PF_6^- and SbF_6^- (73 and 83 Å^3). Thus, across the entire series of anions (Cl^- to SbF_6^-), we see a general trend of decreasing affinity for the single helix. This behavior matches Craig's observations[30] with an aryl-triazole 9-mer. In order to rationalize this loss in affinity, we first consider from our work on the cyanostar[108-109, 113-123] and tricarb[124-125] macrocycles that high-affinity binding of large anions is possible on the occasion when there is complementary size matching between the anion and the cavity. We believe this size matching can occur here given that the foldamer can expand its cavity to complement anion size; we verify this expansion using density functional theory (DFT, *vide infra*). Consequently, we attribute the general loss in affinity with anion size to a reduction in the size of the stabilizing π contact area of the overlapping ends of the foldamer.

Table 1. Stability ($K_{1:1}$, β_2) and equilibrium ($K_{2:1}$) constants for anions binding to **F1**$_{tt}$ (MeCN)[a]

Anion	Volume[b] (A^3)	log $K_{1:1}$	log $K_{2:1}$	log β_2	$\Delta G_{K1:1}$ (kJ /mol)	$\Delta G_{K2:1}$ (kJ / mol)	$\Delta G_{\beta 2}$ (kJ / mol)	Cooperativity $\alpha = 4\ K_{2:1} / K_{1:1}$
Cl^-	20	4.2 ± 0.1	-	-	–24 ± 1	-	-	-
Br^-	29	4.2 ± 0.2	-	-	–24 ± 1	-	-	-
NO_2^-	33	3.6 ± 0.4	-	-	–21 ± 2	-	-	-
I^-	39	4.3 ± 0.2	-	-	–25 ± 1	-	-	-
NO_3^-	41 ± 1	3.2 ± 0.2	-	-	–18 ± 2	-	-	-
SCN^-	49	3.2 ± 0.6	4.5 ± 1.1	7.7 ± 1.7	–18 ± 3	–26 ± 6	–44 ± 10	80
BF_4^-	53 ± 2	3.7 ± 0.2	5.3 ± 0.6	9.0 ± 0.8	–21 ± 1	–30 ± 3	–51 ± 5	160
ClO_4^-	55 ± 1	2.6 ± 0.1	4.7 ± 0.2	7.3 ± 0.1	–15 ± 1	–27 ±1	–42 ± 1	500
ReO_4^-	60 ± 2	2.1 ± 0.1	4.0 ± 1.0	6.1 ± 1.0	–12 ± 1	–23 ± 6	–35 ± 6	320
PF_6^-	73 ± 2	2.8 ± 0.2	3.9 ± 0.2	6.7 ± 0.2	–16 ± 1	–22 ± 1	–38 ± 1	50
SbF_6^-	83 ± 1	1.6 ± 0.3	5.0 ± 0.2	6.6 ± 0.3	–9 ± 2	–29 ± 1	–38 ± 2	10,000

[a]Binding constants determined from UV-Vis titrations. Errors represent the range of variation observed during replicate titrations. [b]Volume method determination can be found in the Supporting Information §S15.

The overall stability of the 2:1 double helical complexes (β_2, Table 1) is highest with tetrafluoroborate (BF_4^-; log $\beta_2 = 9.0 \pm 0.8$). Given that BF_4^- is one of the smallest anions to form a double helix, it has one of the largest equilibrium constants for formation of the single helix (log $K_{1:1} = 3.7 \pm 0.2$). At the same time, the stepwise equilibrium describing the intertwining of a free foldamer with the 1:1 complex ($K_{2:1}$, Table 1) is seen to be almost invariant across the series of anions. As a consequence, the largest double helix stability seen with BF_4^- results from the product of high 1:1 stability and the nearly constant equilibrium associated with foldamer intertwining ($K_{2:1}$). Across the rest of the anions we see a drop of almost three orders of magnitude in stability (β_2), which largely follows $K_{1:1}$.

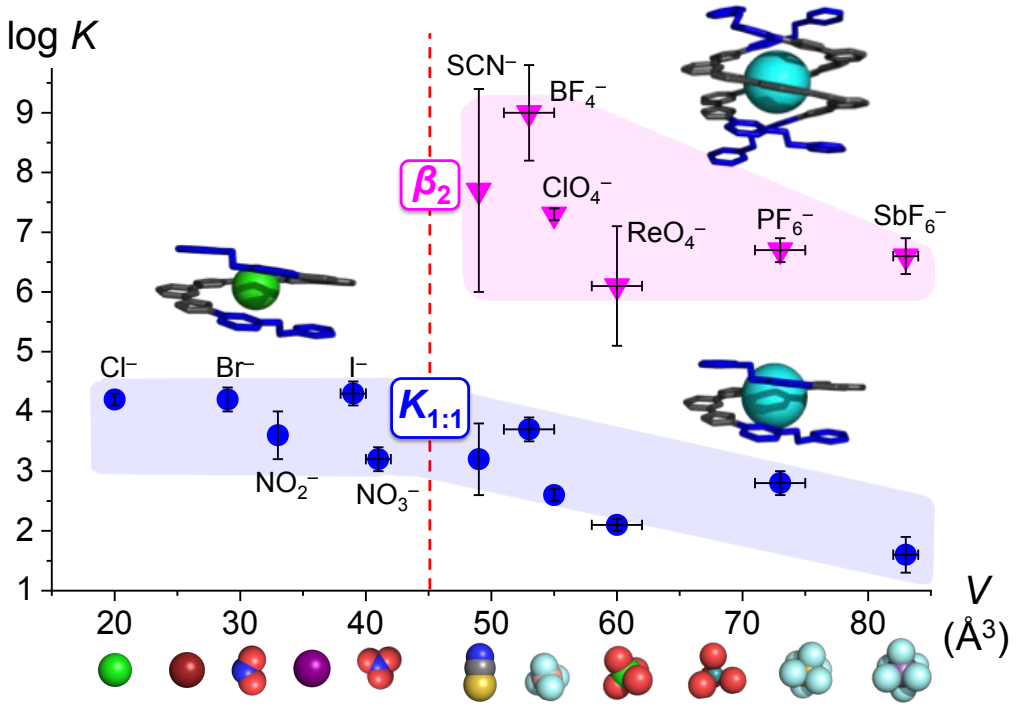

Figure 5. Plot of equilibrium constants, log $K_{1:1}$ (blue), and log β_2 (pink), between various anions towards foldamer $\mathbf{F1}_{tt}$ in acetonitrile against increasing volume size. Anions titrated as TBA^+ salts. Binding constants determined from titrations conducted at foldamer concentrations ranging from 2–300 μM. Binding affinity errors represent the range of variation observed during replicate titrations. Volume errors represent errors in anion volume determination (Table S17).

All the double helical complexes show high positive cooperativity ($\alpha >> 1.0$), ranging 50 to 10,000. Thus, the binding of the first foldamer to the anion provides a significant enhancement for the binding and intertwining of the second foldamer. This effect arises from the fact that, with $K_{2:1}$ remaining fairly constant, the decrease in $K_{1:1}$ with increasing anion size leads to greater cooperativity and, consequently, the dominance of double helices with larger anions. This outcome was rationalized structurally with the aid of DFT-optimized geometries.

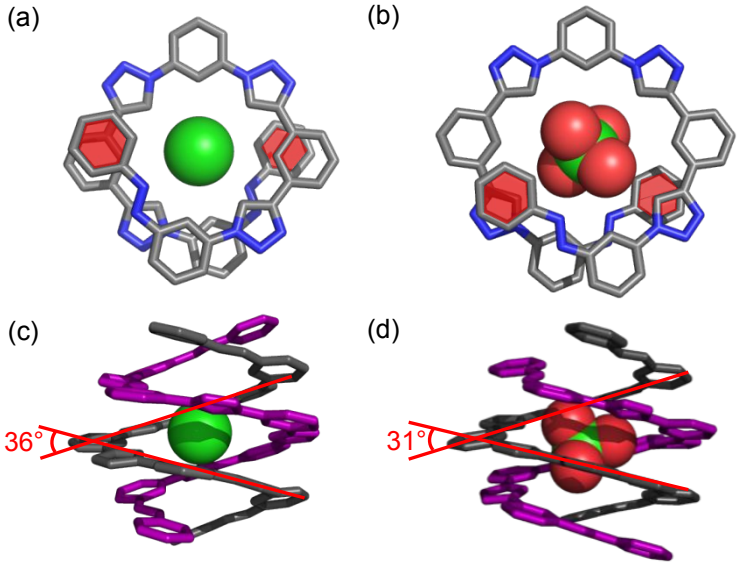

Figure 6. DFT-optimized geometries using ONIOM (B97D3/6-311+G(d):B97D3/6-31G(d)): Top view of the single helix formed around (a) chloride and (b) perchlorate. Side view of calculated double helices around (c) chloride (experimentally unobserved) and (d) perchlorate.

Three Ways that Larger Anions Stabilize Double Helices. To help rationalize the size-dependent preferences in double helix formation (Figure 5), we used DFT to calculate the optimized geometries (Figure 6) of the single and double helices formed around chloride and perchlorate. As the anion size increases from Cl^- (20 Å^3) to ClO_4^- (55 Å^3), we see the cavity for the single helix expands from 5.4 to 6.6 Å (H^D•••H^D distance between OTg-substituted phenylenes). To accommodate the expansion, the overlapping ends of the foldamer have

undergone a sliding motion of the π surfaces with the number of residues per turn increasing from seven (Cl^-) to eight (ClO_4^-). Thus, the size of the π contact area defined by the overlapping arms is reduced. This difference is expected to weaken the stability of the 1:1 helix with perchlorate relative to chloride, correlating with the observed general trend with anion size. The impact of π overlap area on affinity matches our design used here, and elsewhere,[23, 32] to control the number of π contacts and thus anion affinity with azobenzene photoisomerization.

We analyzed the underlying factors contributing to the differences between the single and double helix formation. First, the number of short hydrogen bonds (Table S2) correlates with helix preferences. With chloride, the double helix shows lengthening of all CH•••Cl^- hydrogen bonds; from having six that are less than 2.8 Å in the single helix to all of them being longer than 2.8 Å. With perchlorate, the opposite trend is observed. The number of short hydrogen bonds increases from six to eight on going to the double helix. This structural analysis suggests that enhanced hydrogen bonding favor the single helix with chloride and the double helix with perchlorate.

Second, torsion angles also contribute to helix selection. The double helix around chloride (Figure 6c), which is not observed experimentally, is calculated to have a larger tilt angle (36°) than perchlorate (31°, Figure 6d), which corresponds to increased aryl-triazole torsion angles (Table S3). Larger torsion angles come at an energetic cost.[126] The double helix requires an average 2° change in each torsion angle for perchlorate, whereas chloride requires a larger 5° change (Table S3). The smaller geometrical distortions help favor formation of double helices[64] with larger anions.

Third, the amount of π stacking surface area also enhances stabilization of the double helix. Huc has shown[64] that larger π stacking areas assist stabilization of double helices. Solvent

quality also enhances this stability.[4] In the single helix, the π stacking surface area (Table S5, Figure 6) is larger around chloride (202 Å^2) than perchlorate (169 Å^2). For the double helices, there is an increase in the π stacking surface area relative to two single helices of 1.8 and 2.2 for chloride and perchlorate, respectively (Table S5). Consequently, perchlorate binding in the double helix results in the burial of ~15% more π surface area than for chloride.

In sum, the calculated structures support our observations. The double helix formed around perchlorate shows an increase in the number of short H-bonds and a smaller energetic cost to accommodate the torsion angles relative to the single helix. We also see a larger increase in the π contact area for perchlorate relative to the areal change seen with chloride, consistent with their different helical preferences. In contrast, the formation of the double helix around Cl^- results in a decrease in the number of short H-bonds and larger energetic penalties with larger torsion angles relative to the single helix. These structural differences are consistent with perchlorate favoring the double helix and chloride favoring the single helix.

We also calculated the relative stabilities of the single and double helices in the gas phase (Table S6). We approximated the starting state of the foldamer as a prefolded helix despite the likely existence of multiple accessible conformational states.[127] We also omitted solvation effects. Both the conformations and the impact of solvent on conformational distributions are complex topics of ongoing investigation and outside the scope of our current analysis. Within these limitations, we calculated (§S9) that formation of the double helix with chloride and perchlorate have negative and positive cooperativity, respectively, consistent with experiment.

Selectivity and Anion Affinity of F1$_{UV\text{-}PSS}$. After evaluating the impact of anion size on the binding affinity and structure of the *trans-trans* state of the foldamer, we characterize the allosteric control over function of the photofoldamer. The light-switched UV-PSS contains a

mixture of the *trans-trans*, *cis-trans*, and *cis-cis* isomers in the ratio 16:29:55, respectively (Fig. S84). We did not observe double helix formation for any of the three isomers in a ^{1}H NMR titration with TBACl (Fig. S85) consistent with the behavior of the pure *trans-trans* state.

In order to observe formation of the double helix in the UV photostationary state, a ^{1}H NMR titration was conducted with $TBAClO_4$ (1 mM, 20:80 CD_3CN:CD_2Cl_2). As a means to track all three isomers simultaneously, we conducted the titration on a solution composed of a 1:1:1 ratio of each isomer (Fig. S87). No inflection points were observed (Fig. S88) for the *cis-cis* isomer, indicative of it only forming a single helix. As anticipated from earlier titrations (Figures 4b and 4c), the *trans-trans* isomer showed double helix formation with an inflection point seen at 20 equivalents with proton H^H but not for any of the other protons. Hence, double helix formation appears to be hindered within the isomeric mixture. The *cis-trans* isomer can also participate in a double helix with protons H^H and H^I having inflection points at 10 and 4 equivalents, respectively. In the absence of inflection points for any other internal protons (H^A, H^B, H^C, H^D) of the *cis-trans* isomer, the formation of a double helix is assumed to be of low abundance. Additionally, it is unknown if the double helices are homo- or heterodimers (*tt:tt*, *tt:ct, ct:ct*). As a result of weak double helix stabilities, along with the *cis-cis* isomer constituting 55% of the isomeric solution, the binding affinities in the UV-PSS determined by analysis of the UV-Vis titrations (§S12) in acetonitrile were approximated by an averaged 1:1 binding model.

Our analysis of the binding data show that the unorganized state of the foldamer, $\mathbf{F1}_{\text{UV-PSS}}$, shows no clear anion selectivity (Figure 7). This is surprising given the wide range in anion sizes. However, it is consistent with the low anion selectivity previously observed by Jiang[31] when binding anions spanning 20 to 63 Å^3 in volume to a single helix. Presumably, the cavity of the poorly organized foldamer, $\mathbf{F1}_{\text{UV-PSS}}$, expands to accommodate larger anions instead of

recruiting a second foldamer to stabilize such anions. The steric bulk of the *cis* isomers likely also inhibit formation of the double helix.

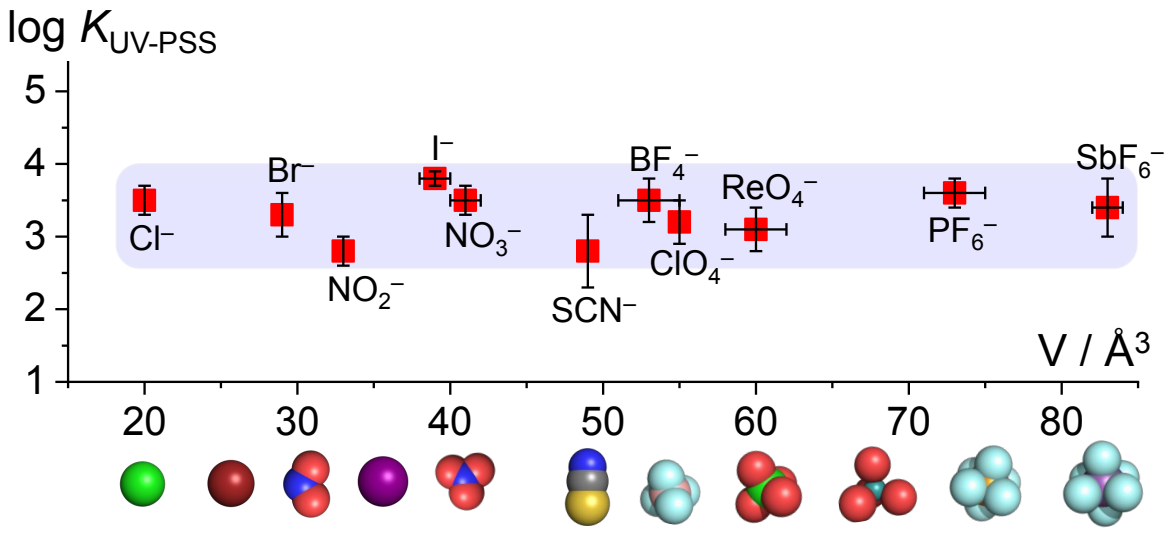

Figure 7. Binding constants (log *K*) of various anions towards foldamer $\mathbf{F1}_{UV-PSS}$ in acetonitrile plotted against increasing volume size. Anions titrated as the TBA^+ salts. Binding constants determined from titrations ranging from 5-100 μM. Binding affinity errors represent the range of variation observed during replicate titrations. Volume errors represent errors in anion volume determination (Table S17).

Allosteric Control of the Function of Photofoldamers using Anions of Different Sizes. With the discovery that small and large anions drive formation of different structures of the photofoldamers, we then considered their different functions. Small anions lead to photodriven binding and release of anions, while large anions enable photoswitching of the quaternary structure by interconverting between chiral double helices and racemic single helices. To highlight how the two functions are different from each other, we selected the working conditions in our experiments. Our selection of different working conditions is no different from the natural changes in the state of a cell, such as, between anabolic and catabolic states after eating and during fasting, respectively. These changes lead to variations in the local

concentrations of effectors to produce different allosteric effects, which we mimic with the foldamer by altering local concentrations of different anions.

The small anions form a single helix that can bind and release anions upon photoirradiation,[23] which is evaluated here across a broader range of anions for the first time (Cl^-, Br^-, I^-, NO_2^-, and NO_3^-). For these anions, the affinity swing is defined as the ratio of the two binding constants ($K_{1:1}$ / $K_{UV\text{-}PSS}$). The largest affinity swing of 8-fold is seen with bromide (29 $Å^3$) and the affinity swings decrease from there: NO_2^- 6× (33 $Å^3$), Cl^- 5× (20 $Å^3$), and I^- 3× (39 $Å^3$). Surprisingly, NO_3^- was found to have an inverse affinity swing of ½× such that the UV-PSS binds the nitrate anion stronger than the *trans-trans* conformation. This outcome likely results from poor shape matching between the *trans-trans* conformation and the trigonal planar nitrate leading to weaker binding than to the *cis*-dominated UV-PSS.

As a read-out of the binding and release of the anions,[23] we measured the conductivity of a salt solution composed of the foldamer and one equivalent of TBACl (Table S12). The conductivity depends on the diffusion coefficient and concentration of all ions in solution. The difference in Cl^- binding strengths between $\mathbf{F1}_{tt}$ (log K = 4.2 ± 0.1) and $\mathbf{F1}_{UV\text{-}PSS}$ (log K = 3.5 ± 0.1) changes the concentration of free Cl^- ions in solution (Fig. S100) and, thus, solution conductivity. A 1 mM solution of **F1** displays the largest affinity swing in the presence of 1 equivalent of TBACl (Figure 8a) and was therefore chosen as the working condition best suited to display the function. The chloride can be reversibly bound and released (Figure 8b) as observed from the cycles in conductivity (Figure 8c) using 365 and 430 nm light to break and remake the binding pocket, respectively, upon light-driven isomerization of the azobenzene.

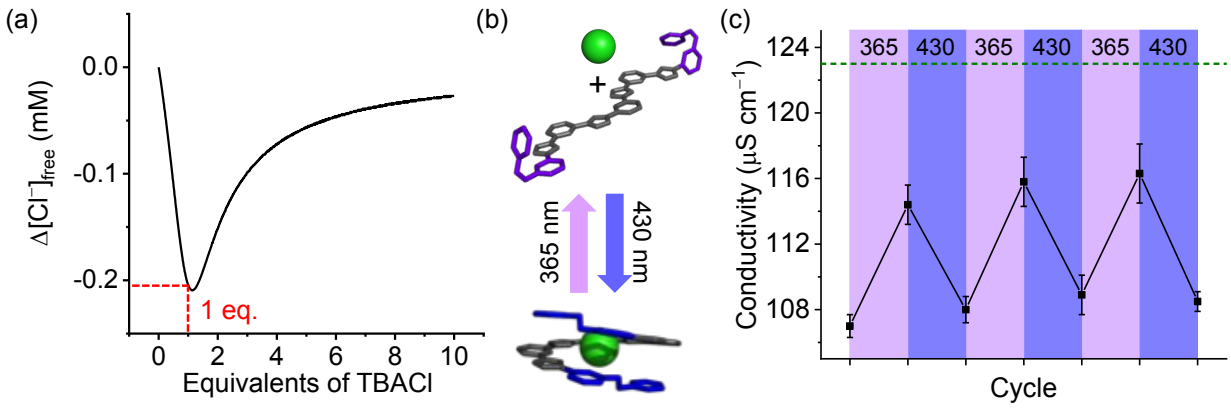

Figure 8. (a) Change in the concentration of free chloride ($\Delta[Cl^-]_{free}$) between the binding (**F1**$_{tt}$) and release (**F1**$_{UVPSS}$) states of **F1** ($\Delta[Cl^-]_{free}$ = *tt*$[Cl^-]_{free}$ – UVPSS$[Cl^-]_{free}$), (b) mechanism of photoswitching, and (c) change in conductivity of a solution of **F1** (1 mM, MeCN, 293-295 K) with 1 equivalent of TBACl as controlled using light. The dashed line corresponds to the conductivity of TBACl (1 mM) sans receptor.

The second function involves reversible chiroptical switching of the quaternary structure between double and single helices, where we use light as a non-destructive and non-invasive stimulus for the first time and read out the change in optical activity. Other stimuli, like acid-base[84] and the activator-inhibitor[85] approach, have been used but they accumulate by-products, thus reducing the life cycle of the systems. We have shown earlier that the double helix is favored with BF_4^- (Figure 5) while the single helix is favored in the UV-PSS (Figure 7). There is also the potential for the double to single helix conversion to produce changes in the concentration of free anions in solution. However, under the working conditions we used, the change in anion concentrations is shown from the binding constants (Fig. S102) to be minimal. Instead, this condition produces the largest change in quaternary structure and corresponding optical activity.

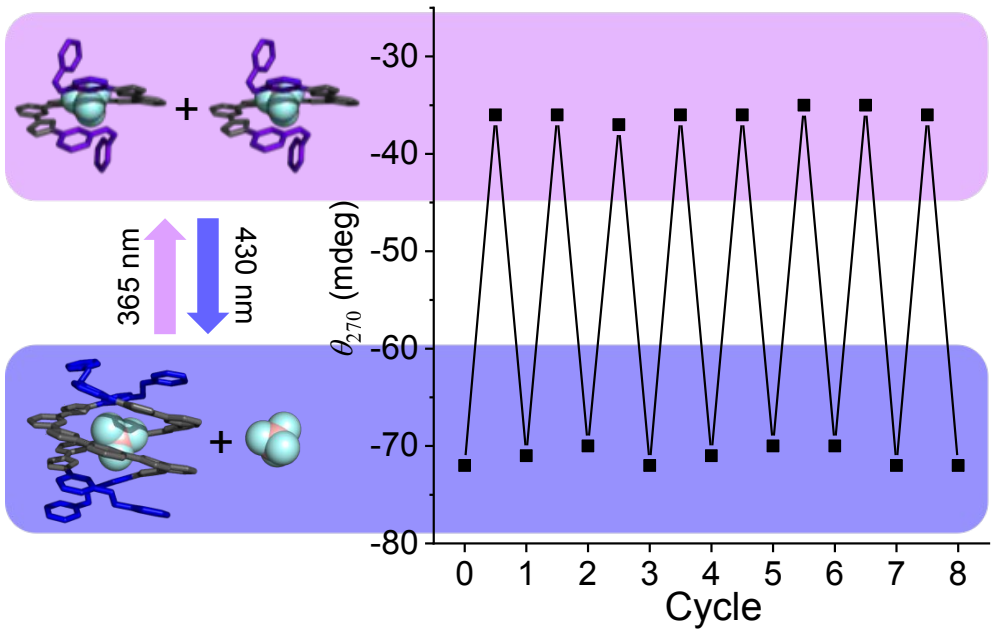

Figure 9. Change in CD response controlled using photoisomerization (**F1**, 0.5 mM, 0.05 cm cuvette, 2 equivalents $TBABF_4$, MeCN, 298 K).

The photoswitching between chiral double helices and racemic single helices was observed using CD spectroscopy (Fig. S101). Upon the addition of 2 equivalents of $TBABF_4$, a solution dominated by the double helix is produced with a corresponding large CD response (Fig. S101). Isomerization with 365 nm light, converts *trans* isomers to *cis* to produce a solution dominated by CD-silent single helices resulting in a decrease in the CD response (Figure 9). Residual CD response correlates with residual double helices. Replicate experiments with 0.5 and 1 equivalents reproduced the results (Figs. S103, S104).

The double helix can then be reformed from the single helix by isomerization with 430 nm light thus giving rise to a cycle. The double helix to single helix conversion was cycled (Figure 9) several times to verify the reversibility promised by the use of light as a non-destructive and non-invasive stimulus. While the photo-driven swing in *cis* and *trans* ratios and

the binding affinities were not large enough to ensure high fidelity transformations, this is the first example of reversible and repetitive photo switching between double and single helices.

CONCLUSION

We have discovered anions as allosteric regulators whose different sizes control the quaternary structure and corresponding function of anion-binding photofoldamers. With small anions that form single helices, UV and visible light stimulation is used to control the anion's concentration in solution. Larger anions enable light-driven chiroptical switching between hierarchical structures composed of chiral double helices and racemic single helices. This allosteric behavior was built on our discovery that the volumetric size of the guest controls formation of single and double helices. The emergence of guest size as a control parameter appears to rely on the synergistic combination with a poor solvent for driving burial of π surfaces, i.e., the solvophobic effect. With anions of larger size (> 45 $Å^3$) a second foldamer is recruited instead of further expansion of the size of the single helix's cavity. Larger anions favor the double helices over single helices on account of being able to form a greater number of shorter hydrogen bonds, more favorable torsion angles, and burial of a larger π surface. Overall, we describe a bioinspired system that displays allosteric regulation of both the structure and function of an abiological photofoldamer. We believe these findings provide general design principles facilitating the use of guest binding to allosterically regulate the function of a stimuli-responsive foldamer.

ASSOCIATED CONTENT

Experimental procedures, compound characterization and spectra, variable solvent CD, ^{1}H NMR titrations, UV-Vis titrations, CD titrations, mass spectrometry, isomerization experiments, computational calculations, ion-pairing contribution, and the determination of anion volumes supplied as Supporting Information (PDF).

AUTHOR INFORMATION

Corresponding Author

*aflood@indiana.edu

Present Address

†Beckman Institute for Advanced Science and Technology, University of Illinois at Urbana-Champaign, 405 North Mathews Avenue, Urbana, IL 61801, USA.

ACKNOWLEDGMENTS

This work was supported by the Chemical Sciences, Geosciences, and Biosciences Division of the Basic Energy Sciences Program of the US Department of Energy Office of Science (DE-FG02-09ER16068). The authors thank Xinfeng Gao from the Indiana University NMR facility, Jonathan A. Karty from the Indiana University Mass Spectrometry Facility, and John Poehlman from the Indiana University Electronics Instrument Services for support. We also thank Katherine VanDenburgh for helpful discussions.

REFERENCES

1. Hecht, S.; Huc, I., *Foldamers : structure, properties, and applications*. Wiley-VCH: Weinheim, 2007, pp 195-228.

2. Ziach, K.; Chollet, C.; Parissi, V.; Prabhakaran, P.; Marchivie, M.; Corvaglia, V.; Bose, P. P.; Laxmi-Reddy, K.; Godde, F.; Schmitter, J. M.; Chaignepain, S.; Pourquier, P.; Huc, I., Single helically folded aromatic oligoamides that mimic the charge surface of double-stranded B-DNA. *Nat. Chem.* **2018,** *10*, 511-518.

3. Rogers, J. M.; Kwon, S.; Dawson, S. J.; Mandal, P. K.; Suga, H.; Huc, I., Ribosomal synthesis and folding of peptide-helical aromatic foldamer hybrids. *Nat. Chem.* **2018,** *10*, 405-412.

4. Hua, Y. R.; Liu, Y.; Chen, C. H.; Flood, A. H., Hydrophobic Collapse of Foldamer Capsules Drives Picomolar-Level Chloride Binding in Aqueous Acetonitrile Solutions. *J. Am. Chem. Soc.* **2013,** *135*, 14401-14412.

5. Monod, J.; Wyman, J.; Changeux, J. P., On Nature of Allosteric Transitions - a Plausible Model. *J. Mol. Biol.* **1965,** *12*, 88-118.

6. Koshland, D. E.; Nemethy, G.; Filmer, D., Comparison of Experimental Binding Data and Theoretical Models in Proteins Containing Subunits. *Biochemistry* **1966,** *5*, 365-385.

7. Hilser, V. J.; Wrabl, J. O.; Motlagh, H. N., Structural and Energetic Basis of Allostery. *Annu. Rev. Biophys.* **2012,** *41*, 585-609.

8. Cuendet, M. A.; Weinstein, H.; LeVine, M. V., The Allostery Landscape: Quantifying Thermodynamic Couplings in Biomolecular Systems. *J. Chem. Theory. Comput.* **2016,** *12*, 5758-5767.

9. Gianneschi, N. C.; Bertin, P. A.; Nguyen, S. T.; Mirkin, C. A.; Zakharov, L. N.; Rheingold, A. L., A supramolecular approach to an allosteric catalyst. *J. Am. Chem. Soc.* **2003,** *125*, 10508-10509.

10. Yoon, H. J.; Kuwabara, J.; Kim, J. H.; Mirkin, C. A., Allosteric Supramolecular Triple-Layer Catalysts. *Science* **2010,** *330*, 66-69.

11. Raynal, M.; Ballester, P.; Vidal-Ferran, A.; van Leeuwen, P. W. N. M., Supramolecular catalysis. Part 2: artificial enzyme mimics. *Chem. Soc. Rev.* **2014,** *43*, 1734-1787.

12. Blanco, V.; Leigh, D. A.; Marcos, V., Artificial switchable catalysts. *Chem. Soc. Rev.* **2015,** *44*, 5341-5370.

13. Lifschitz, A. M.; Young, R. M.; Mendez-Arroyo, J.; McGuirk, C. M.; Wasielewski, M. R.; Mirkin, C. A., Cooperative Electronic and Structural Regulation in a Bioinspired Allosteric Photoredox Catalyst. *Inorg. Chem.* **2016,** *55*, 8301-8308.

14. Qiao, Y. P.; Zhang, L.; Li, J.; Lin, W.; Wang, Z. Q., Switching on Supramolecular Catalysis via Cavity Mediation and Electrostatic Regulation. *Angew. Chem. Int. Ed.* **2016,** *55*, 12778-12782.

15. Rebek, J.; Costello, T.; Marshall, L.; Wattley, R.; Gadwood, R. C.; Onan, K., Allosteric Effects in Organic-Chemistry - Binding Cooperativity in a Model for Subunit Interactions. *J. Am. Chem. Soc.* **1985,** *107*, 7481-7487.

16. Beer, P. D.; Rothin, A. S., A New Allosteric Bis Crown Ether Ligand That Displays Negative Binding Co-Operativity of the Diquat Dication by the Complexation of a Transition-Metal Guest. *J. Chem. Soc., Chem. Comm.* **1988**, 52-54.

17. Sessler, J. L.; Tomat, E.; Lynch, V. M., Positive homotropic allosteric binding of silver(I) cations in a Schiff base oligopyrrolic macrocycle. *J. Am. Chem. Soc.* **2006,** *128*, 4184-4185.

18. Park, J. S.; Le Derf, F.; Bejger, C. M.; Lynch, V. M.; Sessler, J. L.; Nielsen, K. A.; Johnsen, C.; Jeppesen, J. O., Positive Homotropic Allosteric Receptors for Neutral

Guests: Annulated Tetrathiafulvalene-Calix[4]pyrroles as Colorimetric Chemosensors for Nitroaromatic Explosives. *Chem. Eur. J.* **2010,** *16*, 848-854.

19. Davis, C. M.; Lim, J. M.; Larsen, K. R.; Kim, D. S.; Sung, Y. M.; Lyons, D. M.; Lynch, V. M.; Nielsen, K. A.; Jeppesen, J. O.; Kim, D.; Park, J. S.; Sessler, J. L., Ion-Regulated Allosteric Binding of Fullerenes (C-60 and C-70) by Tetrathiafulvalene-Calix[4]pyrroles. *J. Am. Chem. Soc.* **2014,** *136*, 10410-10417.

20. Clever, G. H.; Punt, P., Cation-Anion Arrangement Patterns in Self-Assembled Pd2L4 and Pd4L8 Coordination Cages. *Acc. Chem. Res.* **2017,** *50*, 2233-2243.

21. Park, J. S.; Sessler, J. L., Tetrathiafulvalene (TTF)-Annulated Calix[4]pyrroles: Chemically and Switchable Systems with Encodable Allosteric Recognition and Logic Gate Functions. *Acc. Chem. Res.* **2018,** *51*, 2400-2410.

22. Le Bailly, B. A. F.; Byrne, L.; Clayden, J., Refoldable Foldamers: Global Conformational Switching by Deletion or Insertion of a Single Hydrogen Bond. *Angew. Chem. Int. Ed.* **2016,** *55*, 2132-2136.

23. Hua, Y. R.; Flood, A. H., Flipping the Switch on Chloride Concentrations with a Light-Active Foldamer. *J. Am. Chem. Soc.* **2010,** *132*, 12838-12840.

24. Kato, H.; Fukuda, T.; Parkison, C.; Mcphie, P.; Cheng, S. Y., Cytosolic Thyroid Hormone-Binding Protein Is a Monomer of Pyruvate-Kinase. *Proc. Natl. Acad. Sci. U.S.A.* **1989,** *86*, 7861-7865.

25. Israelsen, W. J.; Vander Heiden, M. G., Pyruvate kinase: Function, regulation and role in cancer. *Semin. Cell Dev. Biol.* **2015,** *43*, 43-51.

26. Morgan, H. P.; O'Reilly, F. J.; Wear, M. A.; O'Neill, J. R.; Fothergill-Gilmore, L. A.; Hupp, T.; Walkinshaw, M. D., M2 pyruvate kinase provides a mechanism for nutrient

sensing and regulation of cell proliferation. *Proc. Natl. Acad. Sci. U.S.A.* **2013,** *110*, 5881-5886.

27. Gao, X. L.; Wang, H. Z.; Yang, J. J.; Chen, J.; Jie, J.; Li, L. W.; Zhang, Y. W.; Liu, Z. R., Reciprocal Regulation of Protein Kinase and Pyruvate Kinase Activities of Pyruvate Kinase M2 by Growth Signals. *J. Biol. Chem.* **2013,** *288*, 15971-15979.

28. Gao, X. L.; Wang, H. Z.; Yang, J. J.; Liu, X. W.; Liu, Z. R., Pyruvate Kinase M2 Regulates Gene Transcription by Acting as a Protein Kinase. *Mol Cell* **2012,** *45*, 598-609.

29. Ashizawa, K.; Cheng, S. Y., Regulation of Thyroid-Hormone Receptor-Mediated Transcription by a Cytosol Protein. *Proc. Natl. Acad. Sci. U.S.A.* **1992,** *89*, 9277-9281.

30. Juwarker, H.; Lenhardt, J. M.; Castillo, J. C.; Zhao, E.; Krishnamurthy, S.; Jamiolkowski, R. M.; Kim, K. H.; Craig, S. L., Anion Binding of Short, Flexible Aryl Triazole Oligomers. *J. Org. Chem.* **2009,** *74*, 8924-8934.

31. Zhao, W.; Huang, F.; Wang, Y.; Li, Q. L.; Shang, J.; Che, Y. K.; Jiang, H., Aryl-triazole foldamers with ethynyl spacers as effective receptors for halides and oxyanions. *Tetrahedron Lett.* **2016,** *57*, 1691-1694.

32. Lee, S.; Hua, Y. R.; Flood, A. H., *β*-Sheet-like Hydrogen Bonds Interlock the Helical Turns of a Photoswitchable Foldamer To Enhance the Binding and Release of Chloride. *J. Org. Chem.* **2014,** *79*, 8383-8396.

33. Khan, A.; Kaiser, C.; Hecht, S., Prototype of a photoswitchable foldamer. *Angew. Chem. Int. Ed.* **2006,** *45*, 1878-1881.

34. Khan, A.; Hecht, S., Towards photocontrol over the helix-coil transition in foldamers: Synthesis and photoresponsive Behavior of azobenzene-core Amphiphilic oligo(meta-phenylene ethynylene)s. *Chem. Eur. J.* **2006,** *12*, 4764-4774.

35. Yu, Z. L.; Hecht, S., Cooperative Switching Events in Azobenzene Foldamer Denaturation. *Chem. Eur. J.* **2012,** *18*, 10519-10524.

36. Yu, Z. L.; Hecht, S., Control over Unfolding Pathways by Localizing Photoisomerization Events within Heterosequence Oligoazobenzene Foldamers. *Angew. Chem. Int. Ed.* **2013,** *52*, 13740-13744.

37. Wang, Y.; Bie, F. S.; Jiang, H., Controlling Binding Affinities for Anions by a Photoswitchable Foldamer. *Org. Lett.* **2010,** *12*, 3630-3633.

38. Yu, Z. L.; Hecht, S., Remote control over folding by light. *Chem. Commun.* **2016,** *52*, 6639-6653.

39. Steinwand, S.; Yu, Z. L.; Hecht, S.; Wachtveitl, J., Ultrafast Dynamics of Photoisomerization and Subsequent Unfolding of an Oligoazobenzene Foldamer. *J. Am. Chem. Soc.* **2016,** *138*, 12997-13005.

40. Mazzier, D.; Crisma, M.; De Poli, M.; Marafon, G.; Peggion, C.; Clayden, J.; Moretto, A., Helical Foldamers Incorporating Photoswitchable Residues for Light-Mediated Modulation of Conformational Preference. *J. Am. Chem. Soc.* **2016,** *138*, 8007-8018.

41. De Poli, M.; Zawodny, W.; Quinonero, O.; Lorch, M.; Webb, S. J.; Clayden, J., Conformational photoswitching of a synthetic peptide foldamer bound within a phospholipid bilayer. *Science* **2016,** *352*, 575-580.

42. Koumura, N.; Zijlstra, R. W. J.; van Delden, R. A.; Harada, N.; Feringa, B. L., Light-driven monodirectional molecular rotor. *Nature* **1999,** *401*, 152-155.

43. Raymo, F. M.; Tomasulo, M., Fluorescence modulation with photochromic switches. *J Phys Chem A* **2005,** *109*, 7343-7352.

44. Siewertsen, R.; Neumann, H.; Buchheim-Stehn, B.; Herges, R.; Nather, C.; Renth, F.; Temps, F., Highly Efficient Reversible Z-E Photoisomerization of a Bridged Azobenzene with Visible Light through Resolved $S_1(n\pi^*)$ Absorption Bands. *J. Am. Chem. Soc.* **2009,** *131*, 15594-+.

45. Weston, C. E.; Richardson, R. D.; Haycock, P. R.; White, A. J. P.; Fuchter, M. J., Arylazopyrazoles: Azoheteroarene Photoswitches Offering Quantitative Isomerization and Long Thermal Half-Lives. *J. Am. Chem. Soc.* **2014,** *136*, 11878-11881.

46. Irie, M.; Fulcaminato, T.; Matsuda, K.; Kobatake, S., Photochromism of Diarylethene Molecules and Crystals: Memories, Switches, and Actuators. *Chem Rev* **2014,** *114*, 12174-12277.

47. Aprahamian, I., Hydrazone switches and things in between. *Chem. Commun.* **2017,** *53*, 6674-6684.

48. Shimasaki, T.; Kato, S. I.; Ideta, K.; Goto, K.; Shinmyozu, T., Synthesis and structural and photoswitchable properties of novel chiral host molecules: Axis chiral 2,2 '-dihydroxy-1,1 '-binaphthyl-appended stiff-stilbene. *J. Org. Chem.* **2007,** *72*, 1073-1087.

49. Li, Z. Y.; Zhang, C.; Ren, Y. L.; Yin, J.; Liu, S. H., Amide- and Urea-Functionalized Dithienylethene: Synthesis, Photochromism, and Binding with Halide Anions. *Org. Lett.* **2011,** *13*, 6022-6025.

50. Han, M. X.; Michel, R.; He, B.; Chen, Y. S.; Stalke, D.; John, M.; Clever, G. H., Light-Triggered Guest Uptake and Release by a Photochromic Coordination Cage. *Angew. Chem. Int. Ed.* **2013,** *52*, 1319-1323.

51. Dabrowa, K.; Niedbala, P.; Jurczak, J., Anion-tunable control of thermal Z -> E isomerisation in basic azobenzene receptors. *Chem. Commun.* **2014,** *50*, 15748-15751.

52. Choi, Y. R.; Kim, G. C.; Jeon, H. G.; Park, J.; Namkung, W.; Jeong, K. S., Azobenzene-based chloride transporters with light-controllable activities. *Chem. Commun.* **2014,** *50*, 15305-15308.

53. Wezenberg, S. J.; Vlatkovic, M.; Kistemaker, J. C. M.; Feringa, B. L., Multi-State Regulation of the Dihydrogen Phosphate Binding Affinity to a Light- and Heat-Responsive Bis-Urea Receptor. *J. Am. Chem. Soc.* **2014,** *136*, 16784-16787.

54. Cafeo, G.; Kohnke, F. H.; Mezzatesta, G.; Profumo, A.; Rosano, C.; Villari, A.; White, A. J. P., Host-Guest Chemistry of a Bis-Calix[4]pyrrole Derivative Containing a trans/cis-Switchable Azobenzene Unit with Several Aliphatic Bis-Carboxylates. *Chem. Eur. J.* **2015,** *21*, 5323-5327.

55. Dabrowa, K.; Niedbala, P.; Jurczak, J., Engineering Light-Mediated Bistable Azobenzene Switches Bearing Urea D-Aminoglucose Units for Chiral Discrimination of Carboxylates. *J. Org. Chem.* **2016,** *81*, 3576-3584.

56. Yuan, Y. X.; Wang, L.; Han, Y. F.; Li, F. F.; Wang, H. B., A novel azo-thiourea based visible light switchable anion receptor. *Tetrahedron Lett.* **2016,** *57*, 878-882.

57. Wezenberg, S. J.; Feringa, B., Photocontrol of Anion Binding Affinity to a Bis-urea Receptor Derived from Stiff-Stilbene. *Org. Lett.* **2017,** *19*, 324-327.

58. Lehn, J. M.; Rigault, A.; Siegel, J.; Harrowfield, J.; Chevrier, B.; Moras, D., Spontaneous Assembly of Double-stranded Helicates from Oligobipyridine Ligands and Copper(I) Cations - Structure of an Inorganic Double Helix. *Proc. Natl. Acad. Sci. U.S.A.* **1987,** *84*, 2565-2569.

59. Berl, V.; Huc, I.; Khoury, R. G.; Krische, M. J.; Lehn, J. M., Interconversion of single and double helices formed from synthetic molecular strands. *Nature* **2000,** *407*, 720-723.

60. Hashimoto, T.; Nishimura, T.; Lim, J. M.; Kim, D.; Maeda, H., Formation of Metal-Assisted Stable Double Helices in Dimers of Cyclic Bis-Tetrapyrroles that Exhibit Spring-Like Motion. *Chem. Eur. J.* **2010,** *16*, 11653-11661.

61. Nelson, J. C.; Saven, J. G.; Moore, J. S.; Wolynes, P. G., Solvophobically driven folding of nonbiological oligomers. *Science* **1997,** *277*, 1793-1796.

62. Lahiri, S.; Thompson, J. L.; Moore, J. S., Solvophobically driven pi-stacking of phenylene ethynylene macrocycles and oligomers. *J. Am. Chem. Soc.* **2000,** *122*, 11315-11319.

63. Goto, H.; Katagiri, H.; Furusho, Y.; Yashima, E., Oligoresorcinols fold into double helices in water. *J. Am. Chem. Soc.* **2006,** *128*, 7176-7178.

64. Berni, E.; Kauffmann, B.; Bao, C. Y.; Lefeuvre, J.; Bassani, D. M.; Huc, I., Assessing the mechanical properties of a molecular spring. *Chem. Eur. J.* **2007,** *13*, 8463-8469.

65. Goto, H.; Furusho, Y.; Miwa, K.; Yashima, E., Double Helix Formation of Oligoresorcinols in Water: Thermodynamic and Kinetic Aspects. *J. Am. Chem. Soc.* **2009,** *131*, 4710-4719.

66. Miwa, K.; Furusho, Y.; Yashima, E., Ion-triggered spring-like motion of a double helicate accompanied by anisotropic twisting. *Nat. Chem.* **2010,** *2*, 444-449.

67. Yamamoto, S.; Iida, H.; Yashima, E., Guest-Induced Unidirectional Dual Rotary and Twisting Motions of a Spiroborate-Based Double-Stranded Helicate Containing a Bisporphyrin Unit. *Angew. Chem. Int. Ed.* **2013,** *52*, 6849-6853.

68. Stahl, J.; Mohr, W.; de Quadras, L.; Peters, T. B.; Bohling, J. C.; Martin-Alvarez, J. M.; Owen, G. R.; Hampel, F.; Gladysz, J. A., sp carbon chains surrounded by sp(3) carbon

double helices: Coordination-driven self-assembly of wirelike Pt(CC)(n)Pt moieties that are spanned by two P(CH2)(m)P linkages. *J. Am. Chem. Soc.* **2007,** *129*, 8282-8295.

69. Sanchez-Quesada, J.; Seel, C.; Prados, P.; Dalcol, I.; Giralt, E.; de Mendoza, J., Anion helicates: Double strand helical self-assembly of chiral bicyclic guanidinium dimers and tetramers around sulfate templates. *J. Am. Chem. Soc.* **1996,** *118*, 277-278.

70. Haketa, Y.; Maeda, H., From Helix to Macrocycle: Anion-Driven Conformation Control of pi-Conjugated Acyclic Oligopyrroles. *Chem. Eur. J.* **2011,** *17*, 1485-1492.

71. Selvakumar, P. M.; Jebaraj, P. Y.; Sahoo, J.; Suresh, E.; Prathap, K. J.; Kureshy, R. I.; Subramanian, P. S., The first bromide ion directed double helicate and its role in catalysis. *RSC Adv.* **2012,** *2*, 7689-7692.

72. Juwarker, H.; Lenhardt, J. M.; Pham, D. M.; Craig, S. L., 1,2,3-triazole CH•••Cl(-) contacts guide anion binding and concomitant folding in 1,4-diaryl triazole oligomers. *Angew. Chem. Int. Ed.* **2008,** *47*, 3740-3743.

73. Wang, Y.; Xiang, J. F.; Jiang, H., Halide-Guided Oligo(aryl-triazole-amide)s Foldamers: Receptors for Multiple Halide Ions. *Chem. Eur. J.* **2011,** *17*, 613-619.

74. Shang, J.; Si, W.; Zhao, W.; Che, Y. K.; Hou, J. L.; Jiang, H., Preorganized Aryltriazole Foldamers as Effective Transmembrane Transporters for Chloride Anion. *Org. Lett.* **2014,** *16*, 4008-4011.

75. Wang, Y.; Zhao, W.; Bie, F. S.; Wu, L.; Li, X. C.; Jiang, H., Ruthenium(II) Complexes of Aryl Triazole Foldamers as Receptors for Anions. *Chem. Eur. J.* **2016,** *22*, 5233-5242.

76. Borissov, A.; Lim, J. Y. C.; Brown, A.; Christensen, K. E.; Thompson, A. L.; Smith, M. D.; Beer, P. D., Neutral iodotriazole foldamers as tetradentate halogen bonding anion receptors. *Chem. Commun.* **2017,** *53*, 2483-2486.

77. Kim, U. I.; Suk, J. M.; Naidu, V. R.; Jeong, K. S., Folding and Anion-Binding Properties of Fluorescent Oligoindole Foldamers. *Chem. Eur. J.* **2008,** *14*, 11406-11414.

78. Suk, J. M.; Jeong, K. S., Indolocarbazole-based foldamers capable of binding halides in water. *J. Am. Chem. Soc.* **2008,** *130*, 11868-11869.

79. Naidu, V. R.; Kim, M. C.; Suk, J. M.; Kim, H. J.; Lee, M.; Sim, E.; Jeong, K. S., Biased Helical Folding of Chiral Oligoindole Foldamers. *Org. Lett.* **2008,** *10*, 5373-5376.

80. Kim, D. A.; Kang, P.; Choi, M. G.; Jeong, K. S., A chiral indolocarbazole foldamer displaying strong circular dichroism responsive to anion binding. *Chem. Commun.* **2013,** *49*, 9743-9745.

81. Jeon, H. G.; Jang, H. B.; Kang, P.; Choi, Y. R.; Kim, J.; Lee, J. H.; Choi, M. G.; Jeong, K. S., Helical Aromatic Foldamers Functioning as a Fluorescence Turn-on Probe for Anions. *Org. Lett.* **2016,** *18*, 4404-4407.

82. Diemer, V.; Fischer, L.; Kauffmann, B.; Guichard, G., Anion Recognition by Aliphatic Helical Oligoureas. *Chem. Eur. J.* **2016,** *22*, 15684-15692.

83. Cao, L.; Jiang, R. S.; Zhu, Y. L.; Wang, X. L.; Li, Y. J.; Li, Y. L., Synthesis of 1,2,3-Triazole-4-carboxamide- Containing Foldamers for Sulfate Recognition. *Eur. J. Org. Chem* **2014,** *2014*, 2687-2693.

84. Barboiu, M.; Vaughan, G.; Kyritsakas, N.; Lehn, J. M., Dynamic chemical devices: Generation of reversible extension/contraction molecular motion by ion-triggered single/double helix interconversion. *Chem. Eur. J.* **2003,** *9*, 763-769.

85. Goto, H.; Furusho, Y.; Yashima, E., Supramolecular control of unwinding and rewinding of a double helix of oligoresorcinol using cyclodextrin/adamantane system. *J. Am. Chem. Soc.* **2007,** *129*, 109-112.

86. Sugiura, H.; Amemiya, R.; Yamaguchi, M., Reversible double-helix-random-coil transition process of bis{hexa(ethynylhelicene)}s. *Chem. - Asian J.* **2008,** *3*, 244-260.

87. Saito, N.; Kobayashi, H.; Yamaguchi, M., "Inverse" thermoresponse: heat-induced double-helix formation of an ethynylhelicene oligomer with tri(ethylene glycol) termini. *Chem. Sci.* **2016,** *7*, 3574-3580.

88. von Krbek, L. K. S.; Schalley, C. A.; Thordarson, P., Assessing cooperativity in supramolecular systems. *Chem. Soc. Rev.* **2017,** *46*, 2622-2637.

89. Zhao, W.; Wang, Y.; Shang, J.; Che, Y. K.; Jiang, H., Acid/Base-Mediated Uptake and Release of Halide Anions with a Preorganized Aryl-Triazole Foldamer. *Chem. Eur. J.* **2015,** *21*, 7731-7735.

90. Zill, A. T.; Zimmerman, S. C., A Route to Water-Soluble Molecularly Templated Nanoparticles Using Click Chemistry and Alkyne-Functionalized Hyperbranched Polyglycerol. *Isr. J. Chem.* **2009,** *49*, 71-78.

91. Xie, L. H.; Suh, M. P., High CO2-Capture Ability of a Porous Organic Polymer Bifunctionalized with Carboxy and Triazole Groups. *Chem. Eur. J.* **2013,** *19*, 11590-11597.

92. Rostovtsev, V. V.; Green, L. G.; Fokin, V. V.; Sharpless, K. B., A stepwise Huisgen cycloaddition process: Copper(I)-catalyzed regioselective "ligation" of azides and terminal alkynes. *Angew. Chem. Int. Ed.* **2002,** *41*, 2596-2599.

93. Tornoe, C. W.; Christensen, C.; Meldal, M., Peptidotriazoles on solid phase: 1,2,3 - triazoles by regiospecific copper(I)-catalyzed 1,3-dipolar cycloadditions of terminal alkynes to azides. *J. Org. Chem.* **2002,** *67*, 3057-3064.

94. Zhao, D. H.; Moore, J. S., Reversible polymerization driven by folding. *J. Am. Chem. Soc.* **2002,** *124*, 9996-9997.

95. Sonogashira, K.; Tohda, Y.; Hagihara, N., Convenient Synthesis of Acetylenes - Catalytic Substitutions of Acetylenic Hydrogen with Bromoalkenes, Iodoarenes, and Bromopyridines. *Tetrahedron Lett.* **1975**, 4467-4470.

96. Kurti, L.; Czakó, B., *Strategic applications of named reactions in organic synthesis*. Elsevier: 2005, pp 424-425.

97. Beharry, A. A.; Woolley, G. A., Azobenzene photoswitches for biomolecules. *Chem. Soc. Rev.* **2011,** *40*, 4422-4437.

98. Solvent quality is a term used in polymer chemistry to desribe the affect that solvent has on intermolecular forces. This term has been adopted and widely used to describe the effect of solvents on the folding of foldamers. For the definition of quality of solvent in polymer chemistry see: IUPAC. Compendium of Chemical Technology, 2nd. ed. (the "Gold Book"). Compiled by A. D. McNaught and A. Wilkinson. Blackwell Scientific Publications, Oxford (1997). XML on-line corrected version: http://goldbook.iupac.org (2006-) created by M. Nic, J. Jirat, B. Kosata; updates compiled by A. Jenkins. ISBN 0-9678550-9-8. https://doi.org/10.1351/goldbook. For examples see (a) Nelson, J. C.; Saven, J. G.; Moore, J. S.; Wolynes, P. G., Science, 1997, 277, 1793-1796. (b) Hill, D. J.; Mio, M. J.; Prince, R. B.; Hughes, T. S.; Moore, J. S., Chem. Rev., 2001, 101, 3893-4011.

99. Reichardt, C., Emperical Parameters of Solvent Polarity as Linear Free-energy Relationships. *Angew. Chem. Int. Ed.* **1979,** *18*, 98-110.

100. Smithrud, D. B.; Sanford, E. M.; Chao, I.; Ferguson, S. B.; Carcanague, D. R.; Evanseck, J. D.; Houk, K. N.; Diederich, F., Solvent Effects in Molecular Recognition. *Pure Appl. Chem.* **1990,** *62*, 2227-2236.

101. Ikkanda, B. A.; Iverson, B. L., Exploiting the interactions of aromatic units for folding and assembly in aqueous environments. *Chem. Commun.* **2016,** *52*, 7752-7759.

102. Stone, M. T.; Moore, J. S., A water-soluble m-phenylene ethynylene foldamer. *Org. Lett.* **2004,** *6*, 469-472.

103. Li, Y. J.; Flood, A. H., Pure C-H hydrogen bonding to chloride ions: A preorganized and rigid macrocyclic receptor. *Angew. Chem. Int. Ed.* **2008,** *47*, 2649-2652.

104. Lee, S.; Hua, Y. R.; Park, H.; Flood, A. H., Intramolecular Hydrogen Bonds Preorganize an Aryl-triazole Receptor into a Crescent for Chloride Binding. *Org. Lett.* **2010,** *12*, 2100-2102.

105. Hua, Y. R.; Flood, A. H., Click chemistry generates privileged CH hydrogen-bonding triazoles: the latest addition to anion supramolecular chemistry. *Chem. Soc. Rev.* **2010,** *39*, 1262-1271.

106. Li, Y. J.; Pink, M.; Karty, J. A.; Flood, A. H., Dipole-Promoted and Size-Dependent Cooperativity between Pyridyl-Containing Triazolophanes and Halides Leads to Persistent Sandwich Complexes with Iodide. *J. Am. Chem. Soc.* **2008,** *130*, 17293-17295.

107. Chang, K. J.; Kang, B. N.; Lee, M. H.; Jeong, K. S., Oligoindole-based foldamers with a helical conformation induced by chloride. *J. Am. Chem. Soc.* **2005,** *127*, 12214-12215.

108. Fatila, E. M.; Twum, E. B.; Sengupta, A.; Pink, M.; Karty, J. A.; Raghavachari, K.; Flood, A. H., Anions Stabilize Each Other inside Macrocyclic Hosts. *Angew. Chem. Int. Ed.* **2016,** *55*, 14057-14062.

109. Fatila, E. M.; Twum, E. B.; Karty, J. A.; Flood, A. H., Ion Pairing and Co-facial Stacking Drive High-Fidelity Bisulfate Assembly with Cyanostar Macrocyclic Hosts. *Chem. Eur. J.* **2017,** *23*, 10652-10662.

110. Suk, J. M.; Naidu, V. R.; Liu, X. F.; Lah, M. S.; Jeong, K. S., A Foldamer-Based Chiroptical Molecular Switch That Displays Complete Inversion of the Helical Sense upon Anion Binding. *J. Am. Chem. Soc.* **2011,** *133*, 13938-13941.

111. We note that the complete loss of the CD signal with just one equivalent of chloride is unexpected. Based on the binding constants 50% of the uncomplexed foldamer still remains in solution (Figure 2d), which we would expect to retain about 50% of the CD signal. This outcome suggests that there may be additional non-specific interactions involving salt-induced changes in the solute-solvent interactions as is often seen with the Hofmeister effect; for example, see (a) Hofmeister, F., Zur lehre von der wirkung der saize, Arch. Exp. Pathol. Phar. 1888, 25, 1-30. (b) Cremer, P. S.; Flood, A. H.; Gibb, B. C.; Mobley, D. L., Collaborative routes to clarifying the murky waters of aqueous supramolecular chemistry, Nat. Chem. 2018, 10, 8-16. (c) Gibb, B. C., Supramolecular Assembly and Binding in Aqueous Solution: Useful Tips Regarding the Hofmeister and Hydrophobic Effects, Isr. J. Chem. 2011, 51, 798-806.

112. Griend, D. A. V.; Bediako, D. K.; DeVries, M. J.; DeJong, N. A.; Heeringa, L. P., Detailed spectroscopic, thermodynamic, and kinetic characterization of nickel(II) complexes with 2,2 '-bipyridine and 1,10-phenanthroline attained via equilibrium-restricted factor analysis. *Inorg. Chem.* **2008,** *47*, 656-662.

113. Lee, S.; Chen, C. H.; Flood, A. H., A pentagonal cyanostar macrocycle with cyanostilbene CH donors binds anions and forms dialkylphosphate [3]rotaxanes. *Nat Chem* **2013,** *5*, 704-710.

114. Hirsch, B. E.; Lee, S.; Qiao, B.; Chen, C. H.; McDonald, K. P.; Tait, S. L.; Flood, A. H., Anion-induced dimerization of 5-fold symmetric cyanostars in 3D crystalline solids and 2D self-assembled crystals. *Chem. Commun.* **2014,** *50*, 9827-9830.

115. Qiao, B.; Anderson, J. R.; Pink, M.; Flood, A. H., Size-matched recognition of large anions by cyanostar macrocycles is saved when solvent-bias is avoided. *Chem. Commun.* **2016,** *52*, 8683-8686.

116. Benson, C. R.; Fatila, E. M.; Lee, S.; Marzo, M. G.; Pink, M.; Mills, M. B.; Preuss, K. E.; Flood, A. H., Extreme Stabilization and Redox Switching of Organic Anions and Radical Anions by Large-Cavity, CH Hydrogen-Bonding Cyanostar Macrocycles. *J. Am. Chem. Soc.* **2016,** *138*, 15057-15065.

117. Liu, Y.; Singharoy, A.; Mayne, C. G.; Sengupta, A.; Raghavachari, K.; Schulten, K.; Flood, A. H., Flexibility Coexists with Shape-Persistence in Cyanostar Macrocycles. *J. Am. Chem. Soc.* **2016,** *138*, 4843-4851.

118. Qiao, B.; Liu, Y.; Lee, S. M.; Pink, M.; Flood, A. H., A high-yield synthesis and acid-base response of phosphate-templated[3]rotaxanes. *Chem. Commun.* **2016,** *52*, 13675-13678.

119. Zhao, W.; Qiao, B.; Chen, C. H.; Flood, A. H., High-Fidelity Multistate Switching with Anion-Anion and Acid-Anion Dimers of Organophosphates in Cyanostar Complexes. *Angew. Chem. Int. Ed.* **2017,** *56*, 13083-13087.

120. Qiao, B.; Hirsch, B. E.; Lee, S.; Pink, M.; Chen, C. H.; Laursen, B. W.; Flood, A. H., Ion-Pair Oligomerization of Chromogenic Triangulenium Cations with Cyanostar-Modified Anions That Controls Emission in Hierarchical Materials. *J. Am. Chem. Soc.* **2017,** *139*, 6226-6233.

121. Zahran, E. M.; Fatila, E. M.; Chen, C. H.; Flood, A. H.; Bachas, L. G., Cyanostar: C-H Hydrogen Bonding Neutral Carrier Scaffold for Anion-Selective Sensors. *Anal. Chem.* **2018,** *90*, 1925-1933.

122. Fatila, E. M.; Pink, M.; Twum, E. B.; Karty, J. A.; Flood, A. H., Phosphate-phosphate oligomerization drives higher order co-assemblies with stacks of cyanostar macrocycles. *Chem. Sci.* **2018,** *9*, 2863-2872.

123. Sheetz, E. G.; Qiao, B.; Pink, M.; Flood, A. H., Programmed Negative Allostery with Guest-Selected Rotamers Control Anion-Anion Complexes of Stackable Macrocycles. *J. Am. Chem. Soc.* **2018,** *140*, 7773-7777.

124. Lee, S.; Hirsch, B. E.; Liu, Y.; Dobscha, J. R.; Burke, D. W.; Tait, S. L.; Flood, A. H., Multifunctional Tricarbazolo Triazolophane Macrocycles: One-Pot Preparation, Anion Binding, and Hierarchical Self-Organization of Multilayers. *Chem. Eur. J.* **2016,** *22*, 560-569.

125. Dobscha, J. R.; Debnath, S.; Fadler, R. E.; Fatila, E. M.; Pink, M.; Raghavachari, K.; Flood, A. H., Host-Host Interactions Control Self-assembly and Switching of Triple and Double Decker Stacks of Tricarbazole Macrocycles Co-assembled with *Anti*-electrostatic Bisulfate Dimers. *Chem. Eur. J.* **2018,** *24*, 9841-9852.

126. Li, Y. L.; Flood, A. H., Strong, size-selective, and electronically tunable C-H•••halide binding with steric control over aggregation from synthetically modular, shape-persistent [3(4)]triazolophanes. *J. Am. Chem. Soc.* **2008,** *130*, 12111-12122.

127. Galan, J. F.; Tang, C. N.; Chakrabarty, S.; Liu, Z. W.; Moyna, G.; Pophristic, V., Conformational preferences of furan- and thiophene-based arylamides: a combined computational and experimental study. *Phys Chem Chem Phys* **2013,** *15*, 11883-11892.

TOC GRAPHICAL ABSTRACT